Coordination and Reactivity Diversity of *N*-Piperidineethyl-Functionalized Indenyl Ligands: Synthesis, Structure, Theoretical Calculation, and Catalytic Activity of Organolanthanide Complexes with the Ligands

Shaowu Wang,*[,†,‡] Xinliang Tang,[†] Andres Vega,[§] Jean-Yves Saillard,*[,⊥] Shuangliu Zhou,[†] Gaosheng Yang,[†] Wei Yao,[†] and Yun Wei[†]

Anhui Key Laboratory of Functional Molecular Solids, Institute of Organic Chemistry, School of Chemistry and Materials Science, Anhui Normal University, Wuhu, Anhui 241000, People's Republic of China, State Key Laboratory of Organometallic Chemistry, Shanghai Institute of Organic Chemistry, Shanghai 200032, People's Republic of China, Departamento de Quimica, Facultad de Ecología y Recursos Naturales, Universidad Nacional Andres Bello, Republica 275, Santiago, Chile, and Sciences Chimiques de Rennes, UMR-CNRS 6226, Université de Rennes 1, 35042 Rennes Cedex, France

Received October 24, 2006

The interactions of *N*-piperidineethyl-functionalized indene compounds 1-R-3-$C_5H_{10}NCH_2CH_2C_9H_6$ (R = H− (**1**), Me_3Si− (**2**)) with lanthanide(III) amides $[(Me_3Si)_2N]_3Ln(\mu\text{-Cl})Li(THF)_3$ (Ln = Yb, Eu, Sm, Nd) were studied. The results indicated that the ligands and reductive potentials of Ln^{3+}/Ln^{2+} have an influence on the reaction patterns and the coordination mode of the indenyl ligands with the central metals. Reactions of $[(Me_3Si)_2N]_3Ln(\mu\text{-Cl})Li(THF)_3$ (Ln = Yb, Eu) with 2 equiv of corresponding indene compounds 1-R-3-$C_5H_{10}NCH_2CH_2C_9H_6$ (R = H− (**1**), Me_3Si− (**2**)) produced organolanthanide(II) complexes $[\eta^5{:}\eta^1\text{-}C_5H_{10}NCH_2CH_2C_9H_6]_2Ln^{II}$ (Ln = Yb (**3**), Eu (**5**)) and novel organolanthanide(II) complexes with general formula $[\eta^4{:}\eta^2{:}\eta^1\text{-}(C_5H_{10}NCH_2CH_2C_9H_5SiMe_3)Li(\mu\text{-Cl})]Ln^{II}(\eta^5{:}\eta^1\text{-}C_5H_{10}NCH_2\text{-}CH_2C_9H_5SiMe_3)$ (Ln = Yb (**4**), Eu (**6**)), and a new highly conjugated bis(*N*-piperidineethyl)-dibenzofulvalene, $(C_5H_{10}NCH_2CH_2C_9H_5)_2$ (**9**), was unexpectedly isolated as a byproduct in the preparation of **6**, indicating the ligands' effects on the coordination and reactivity patterns. Theoretical calculations on ytterbium(II) complexes having indenyl ligands indicated that the indenyl hapticity depends on the strain, steric, and electronic effects. Treatment of lanthanide(III) amides $[(Me_3Si)_2N]_3Ln(\mu\text{-Cl})Li(THF)_3$ (Ln = Sm, Nd) with 2 equiv of $C_5H_{10}NCH_2CH_2C_9H_7$ (**1**) afforded indenyl lanthanide(III) complexes with general formula $[\eta^3\text{-}C_5H_{10}NCH_2CH_2C_9H_6]_2Ln^{III}[\eta^3{:}\eta^1\text{-}C_5H_{10}NCH_2CH_2C_9H_6]$ (Ln = Sm (**7**), Nd (**8**)). The shortest distances involving the nonbridging atoms of the C_5 portions of the indenyl groups indicated an allyl-like nature of the ligand-to-metal coordination. The interaction of $[(Me_3Si)_2N]_3Sm^{III}(\mu\text{-Cl})Li\text{-}(THF)_3$ with 2 equiv of 1-Me_3Si-3-$C_5H_{10}NCH_2CH_2C_9H_6$ (**2**) produced an unexpected bis(*N*-piperidineethyl)-dibenzofulvalene $(C_5H_{10}NCH_2CH_2C_9H_5)_2$ (**9**) and other unidentified solids, suggesting the ligands' influence on the reactivity patterns. All the compounds were fully characterized by spectroscopic methods and elemental analyses. The structures of compounds **4**, **7**, **8**, and **9** were additionally determined by X-ray diffraction study. The catalytic activity of the organolanthanide complexes **3**−**8** on MMA polymerization was examined. It was found that the π-bonded tris(*N*-piperidineethylindenyl)lanthanide(III) complexes **7** and **8** exhibit unexpected good catalytic activity on MMA polymerization, and complex **7** also showed an unexpected high catalytic activity on ε-caprolactone polymerization. It was found that the catalytic activity of the complexes depended on the polymerization conditions. The solvents, temperatures, substituted groups, and lanthanide ionic radii effects on the catalytic activity of the complexes were examined.

Introduction

It has been demonstrated that indenyl is a less electron rich, more sterically demanding, yet planar π ligand than cyclopentadienyl.[1] The former can bond either to the transition metals through the C_5 ring with η^1, η^2, η^3, and η^5 hapticity[2] or to the group 4 and group 6 metals through the benzo ring as an η^6 ligand.[3,4] Recently, the η^9 and $\mu\text{-}\eta^4\eta^5$-bridging bonding mode of the indenyl ligand with a transition metal has been reported.[5] It has been proposed that reaction of bis(^{i}Pr-indenyl)$_2$Yb(THF)$_2$ with excess $AlMe_3$ produced an ytterbium(II) complex having the indenyl ligands bonded to the metal through the benzo ring in an η^6 hapticity.[6] However, structural characterization of this

* Corresponding authors. (S.W.) Fax: (+) 86-553-3883517. E-mail: swwang@mail.ahnu.edu.cn. (J.-Y.S.) E-mail: saillard@univ-rennes1.fr.
† Anhui Normal University.
‡ Shanghai Institute of Organic Chemistry.
§ Universidad Nacional Andres Bello.
⊥ Université de Rennes 1.

(1) O'Connor, J. M.; Casey, C. P. *Chem. Rev.* **1987**, *87*, 307.
(2) (a) Sui-Seng, C.; Enright, G. D.; Zargarian, D. *J. Am. Chem. Soc.* **2006**, *128*, 6508−6519. (b) Calhorda, M. J.; Félix, V.; Veiros, L. F. *Coord. Chem. Rev.* **2002**, *230*, 49. (c) Stradiotto, M.; McGlinchey, M. J. *Coord. Chem. Rev.* **2001**, *219*−*221*, 311, and references therein.
(3) (a) Bradley, C. A.; Lobkovsky, E.; Chirik, P. J. *J. Am. Chem. Soc.* **2003**, *125*, 8110. (b) Veiros, L. F. *Organometallics* **2006**, *25*, 4698−4701.
(4) Kubas, G. L.; Kiss, G.; Hoff, C. D. *Organometallics* **1991**, *10*, 2870.

10.1021/om060979i CCC: $37.00
Publication on Web 02/14/2007

type of ytterbium(II) complex remains to be elucidated. The other bonding mode of the indenyl ligands to the metals remains to be reported.

Of the variety of early transition metal-based catalysts for olefin transformation, complexes of the lanthanide amide catalysts appear uniquely well suited for alkene and alkyne hydroamination,[7] hydrosilylation,[8] hydrophosphination,[9] and Tischenko reaction,[10] as well as Cannizarro-type disproportionation and Aldol condensation.[11] It has been proved that the interactions of different heteroatom-functionalized side arm substituted indene compounds with the lanthanide amides produced different kinds of organolanthanide(II) complexes. The interaction of pyrrolidine-functionalized indene compounds with the europium(III) amide $[(Me_3Si)_2N]_3Eu(\mu\text{-}Cl)Li(THF)_3$ produced a novel tetranuclear triple-decker europium(II) complex with a linked indenyl ligand,[12] while the interaction of methoxyethyl-,[13] dimethylaminoethyl-,[14] furfuryl- or tetrahydrofurfuryl, or 2-pyridylmethyl-functionalized[15] indene compounds with lanthanide(III) amides $[(Me_3Si)_2N]_3Ln(\mu\text{-}Cl)Li(THF)_3$ (Ln = Yb, Eu) gave monomeric indenyl organolanthanide(II) complexes via a tandem silylamine elimination/homolysis of the Ln−N bond reaction; thus, the reaction provided a new methodology for the preparation of organolanthanide(II) complexes with indenyl ligands incorporating donor-substituted groups. Meanwhile, evidence that Sm^{3+}/Sm^{2+} and Nd^{3+}/Nd^{2+} ions have more negative reductive potentials than those of Yb^{3+}/Yb^{2+} or Eu^{3+}/Eu^{2+} has been well established;[16] so, it is naturally for us to design or select different sterically demanding indene compounds and to study their interactions with the lanthanide(III) amides $[(Me_3Si)_2N]_3Ln(\mu\text{-}Cl)Li(THF)_3$ (Ln = Yb, Eu, Sm, Nd) to examine steric, electronic, and reductive potentials' effects on the reaction.

Scheme 1

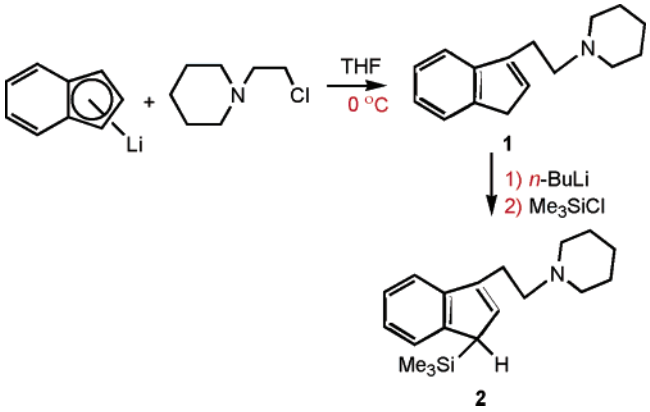

In this paper, we will report the interactions of *N*-piperidineethyl-functionalized indene compounds 1-R-3-$C_5H_{10}NCH_2CH_2C_9H_6$ (R = H− or Me_3Si−) with lanthanide(III) amides $[(Me_3Si)_2N]_3Ln(\mu\text{-}Cl)Li(THF)_3$ (Ln = Yb, Eu, Sm, Nd), leading to the isolation and characterization of the first examples of organolanthanide complexes with indenyl ligands in a novel η^4-bonding mode and the theoretical calculations on the ytterbium(II) complex having a η^4-bonded indenyl ligand. The π-bonded tris-indenyl lanthanide(III) complexes with unexpected good catalytic activity on MMA polymerization and high activity on ϵ-caprolactone polymerization will also be reported. The steric and Ln^{3+}/Ln^{2+} reductive potentials' effects on the reactivity will be discussed in this paper. A portion of this work was previously communicated.[17]

Results and Discussion

Synthesis of the Ligands. The ligand $C_5H_{10}NCH_2CH_2C_9H_7$ (**1**) was prepared by the reaction of freshly prepared indenyl lithium with *N*-piperidineethyl chloride in THF. ^1H NMR spectra indicated that the *N*-piperidineethyl group was connected to the sp^2 carbon of the five-membered ring of indene. Lithiation of **1** with butyl lithium, followed by treatment with excess trimethylsilyl chloride, produced 1-Me_3Si-3-$C_5H_{10}NCH_2CH_2C_9H_6$ (**2**). The compound was fully characterized by NMR spectra and elemental analyses. The synthetic processes are outlined in Scheme 1.

Interaction of *N*-Piperidineethyl-Functionalized Indene Compounds with $[(Me_3Si)_2N]_3Ln(\mu\text{-}Cl)Li(THF)_3$. Synthesis and Characterization of Novel Indenyl Lanthanide Complexes. Treatment of lanthanide(III) amides $[(Me_3Si)_2N]_3Ln(\mu\text{-}Cl)Li(THF)_3$ (Ln = Yb, Eu) with 2 equiv of the corresponding indene compounds 1-R-3-$C_5H_{10}NCH_2CH_2C_9H_6$ (R = H− (**1**), Me_3Si− (**2**)) produced lanthanide(II) complexes $[\eta^5\text{:}\eta^1\text{-}C_5H_{10}NCH_2CH_2C_9H_6]_2Ln^{II}$ (Ln = Yb (**3**); Eu (**5**)) (Scheme 2) and novel organolanthanide(II) complexes with general formula $[\eta^4\text{:}\eta^2\text{:}\eta^1\text{-}(C_5H_{10}NCH_2CH_2C_9H_5SiMe_3)Li(\mu\text{-}Cl)]Ln^{II}(\eta^5\text{:}\eta^1\text{-}C_5H_{10}NCH_2CH_2C_9H_5SiMe_3)$ (Ln = Yb (**4**); Eu (**6**)) (Scheme 3). All complexes were fully characterized by spectroscopic methods

(5) (a) Bradley, C. A.; Keresztes, I.; Lobkovsky, E.; Young, V. G.; Chirik, P. J. *J. Am. Chem. Soc.* **2004**, *126*, 16937. (b) Bradley, C. A.; Lobkovsky, E.; Keresztes, I.; Chirik, P. J. *J. Am. Chem. Soc.* **2006**, *128*, 6454. (c) Veiros, L. F. *Chem.−Eur. J.* **2005**, *11*, 2505. (d) Veiros, L. F. *Organometallics* **2006**, *25*, 2266. (e) Trifonov, A. A.; Fedorova, E. A.; Fukin, G. K.; Baranov, E. V.; Druzhkov, N. O.; Bochkarev, M. N. *Chem.−Eur. J.* **2006**, *12*, 2752.

(6) Nakamura, H.; Nakayama, Y.; Yasuda, H.; Maruo, T.; Kanehisa, N.; Kai, Y. *Organometallics* **2000**, *19*, 5392.

(7) (a) Kim, H.; Livinghouse, T.; Shim, J. H.; Lee, S. G.; Lee, P. H. *Adv. Synth. Catal.* **2006**, *348*, 701−704. (b) Gribkov, D. V.; Hultzsch, K. C.; Hampel, F. *J. Am. Chem. Soc.* **2006**, *128*, 3748−3759. (c) Kim, Y. K.; Livinghouse, T.; Bercaw, J. E. *Tetrahedron Lett.* **2001**, *42*, 2933. (d) Kim, J. Y.; Livinghouse, T. *Org. Lett.* **2005**, *7*, 4391. (e) Kim, J. Y.; Livinghouse, T. *Org. Lett.* **2005**, *7*, 1737. (f) Kim, Y. K.; Livinghouse, T.; Horino, Y. *J. Am. Chem. Soc.* **2003**, *125*, 9560. (g) Kim, Y. K.; Livinghouse, T. *Angew. Chem. Int. Ed.* **2002**, *41*, 3645. (h) Hong, S.; Marks, T. J. *Acc. Chem. Res.* **2004**, *37*, 673. (i) Rastätter, M.; Zulys, A.; Roesky, P. W. *Chem. Commun.* **2006**, 874−876. (j) Bürgstein, M. R.; Berberich, H.; Roesky, P. W. *Organometallics* **1998**, *17*, 1452−1454. (k) Ryu, J. S.; Li, Y. G.; Marks, T. J. *J. Am. Chem. Soc.* **2003**, *125*, 12584−12605.

(8) (a) Horino, Y.; Livinghouse, T. *Organometallics* **2004**, *23*, 12. (b) Gountchev, T. I.; Tilley, T. D. *Organometallics* **1999**, *18*, 5661−5667. (c) Gribkov, D. V.; Hampel, F.; Hultzsch, K. C. *Eur. J. Inorg. Chem.* **2004**, 4091−4101.

(9) (a) Komeyama, K.; Kawabata, T.; Takehira, K.; Takaki, K. *J. Org. Chem.* **2005**, *70*, 7260−7266. (b) Kawaoka, A. M.; Douglass, M. R.; Marks, T. J. *Organometallics* **2003**, *22*, 4630−4632. (c) Takaki, K.; Koshoji, G.; Komeyama, K.; Takeda, M.; Shishido, T.; Kitani, A.; Takehira, K. *J. Org. Chem.* **2003**, *68*, 6554−6565. (d) Douglass, M. R.; Stern, C. L.; Marks, T. J. *J. Am. Chem. Soc.* **2001**, *123*, 10221−10238. (e) Douglass, M. R.; Marks, T. J. *J. Am. Chem. Soc.* **2000**, *122*, 1824−1825.

(10) (a) Berberich, H.; Roesky, P. W. *Angew. Chem., Int. Ed.* **1998**, *37*, 1569. (b) Bürgstein, M. R.; Berberich, H.; Roesky, P. W. *Chem.−Eur. J.* **2001**, *7*, 3078−3085.

(11) (a) Zhang, L.; Wang, S.; Zhou, S.; Yang, G.; Sheng, E. *J. Org. Chem.* **2006**, *71*, 3149. (b) Zhang, L.; Wang, S.; Sheng, E.; Zhou, S. *Green Chem.* **2005**, *7*, 683.

(12) Wang, S.; Zhou, S.; Sheng, E.; Xie, M.; Zhang, K.; Cheng, L.; Feng, Y.; Mao, L.; Huang, Z. *Organometallics* **2003**, *22*, 3546.

(13) Zhang, K.; Zhang, W.; Wang, S.; Sheng, E.; Yang, G.; Xie, M.; Zhou, S.; Feng, Y.; Mao, L.; Huang, Z. *Dalton Trans.* **2004**, 1029.

(14) (a) Sheng, E.; Wang, S.; Yang, G.; Zhou, S.; Cheng, L.; Zhang, K.; Huang, Z. *Organometallics* **2003**, *22*, 684. (b) Sheng, E.; Zhou, S.; Wang, S.; Yang, G.; Wu, Y.; Feng, Y.; Mao, L.; Huang, Z. *Eur. J. Inorg. Chem.* **2004**, 2923.

(15) (a) Wu, Y.; Wang, S.; Qian, C.; Sheng, E.; Xie, M.; Yang, G.; Feng, Q.; Zhang, L.; Tang, X. *J. Organomet. Chem.* **2005**, *690*, 4139. (b) Wang, S.; Feng, Y.; Mao, L.; Sheng, E.; Yang, G.; Xie, M.; Wang, S.; Wei, Y.; Huang, Z. *J. Organomet. Chem.* **2006**, *691*, 1265−1274.

(16) Evans, W. J. *Coord. Chem. Rev.* **2000**, *206−207*, 263.

(17) Wang, S.; Tang, X.; Vega, A.; Saillard, J. Y.; Sheng, E.; Yang, G.; Zhou, S.; Huang, Z. *Organometallics* **2006**, *25*, 2399−2401.

Scheme 2

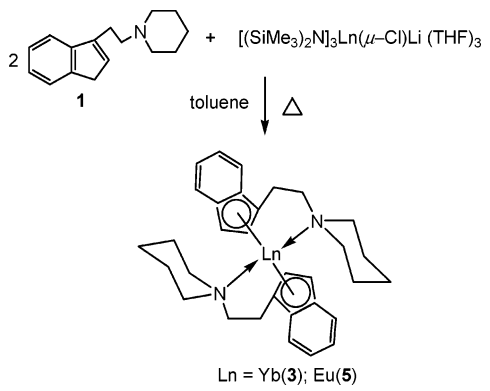

Scheme 3

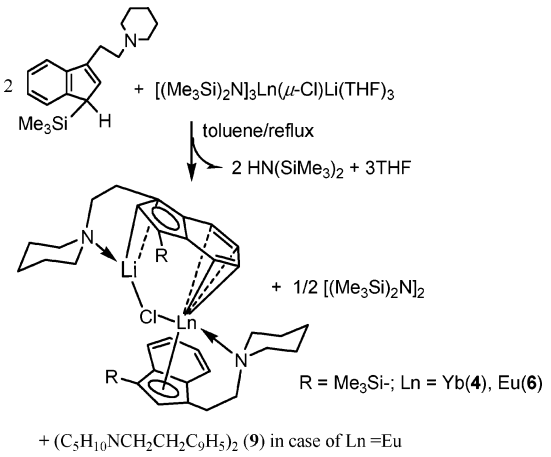

and standard elemental analyses, and the solid-state structure of complex **4** was established by single-crystal X-ray diffraction study. They are extremely sensitive to air and moisture and soluble in polar solvents such as THF, DME, and pyridine. Complexes **5** and **6** are soluble in toluene and benzene, but only slightly soluble in *n*-hexane. Complexes **3** and **4** are only slightly soluble in toluene and insoluble in *n*-hexane.

^{1}H NMR spectra of compounds **3** and **4** showed a diamagnetic property of the complexes, indicating that the oxidation state of the central metals is +2, which has been proved by the solid-state structure of complex **4**. The results suggested that the formation of the complexes goes through a one-electron reductive elimination process. ^{1}H NMR spectra of compound **4** in pyridine-d_5 and in benzene-d_6 gave different chemical shifts for the ligands. In benzene-d_6 the indenyl ligands resonated in the range 9.27 to 6.18 ppm. Two sharp singlets (0.39 and 0.20 ppm) are observed for the two silyl groups, indicating that there are two distinct Me_3Si groups in **4**. However, in pyridine-d_5 the indenyl ligand resonated in the range 8.15 to 6.47 ppm, and only one broad singlet is observed for the two Me_3Si groups. These results suggested that the integrity of complex **4** is retained in a nonpolar solvent such as benzene, whereas it differs in pyridine probably due to coordination of Li^+ and Yb^{2+}. This could lead to dissociation of LiCl from complex **4**. However, attempts to isolate a compound without coordinated LiCl from the pyridine failed.

X-ray analysis revealed that complex **4** shows the first observed bonding mode of the indenyl ligand through a benzo ring in an η^4-fashion and one normally observed bonding mode of the indenyl ligand in an η^5-mode, which represents the first example of a structurally authenticated organolanthanide complex having an indenyl ligand bonded to the central metal through the benzo ring with η^4-hapticity (Figure 1).[1,2]

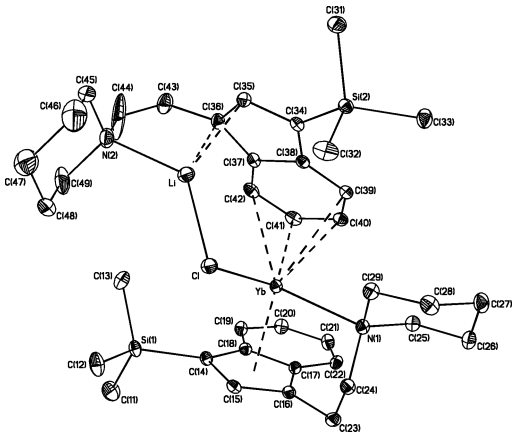

Figure 1. Molecular structure of **4**. Hydrogen atoms are omitted for clarity.

It is found that the Yb−C(C_6 ring) bond distances range from 2.733(6) to 3.221(6) Å, and the corresponding Yb−C(37) and Yb−C(38) distances of 3.221(6) and 3.139(6) Å are significantly longer than the other Yb−C(C_6 ring) distances (Table 1). The Yb−C(39) and Yb−C(42) distances of 2.903(6) and 3.010(7) Å (with an average of 2.956(7) Å) found in **4** are comparable to the average Eu−C distance of 3.002(18) Å found in the η^6-π-arene europium(II) complex $[Eu(C_6Me_6)AlCl_4]_2]_4$,[18] and those of π-arene interaction complexes [Dmp(Tph)N_3MC_6F_5] (M = Eu, Yb; Dmp = 2,6-$Mes_2C_6H_3$ with Mes = 2,4,6-$Me_3C_6H_2$; Tph = 2-TripC_6H_4 with Trip = 2,4,6-^{i}Pr$_3C_6H_2$)[19] and those of assigned η^6-π-arene complexes $M^{II}(SAr^*)_2$ (M = Eu with average Eu−C distances of 3.065(3) Å, M = Yb with average Yb−C distances of 2.973(9) Å; Ar* = 2,6-$Trip_2C_6H_3$ with trip = 2,4,6-^{i}Pr$_3C_6H_2$),[20] if the ionic radii difference between Yb^{2+} and Eu^{2+} with different coordination numbers was taken into account.[21] The Yb−C(40) and Yb−C(41) distances of 2.733(6) and 2.772(6) Å found in **4** are comparable to the Yb−C(μ-C_2H_4) (2.770(3) and 2.793(3) Å) and the Yb−C(η^2-MeC≡CMe) (2.659 ± 0.009 Å) distances found in $(Me_5C_5)_2$Yb(μ-C_2H_4)Pt(PPh_3)[22] and $(Me_5C_5)_2$Yb(η^2-MeC≡CMe),[23] respectively. Therefore, the ligand bonding in **4** is best described as an η^4-bonding on the basis of these structural parameters. The theoretical analysis reported below supports this conclusion. This structure represents the first example of an organolanthanide(II) complex having the indenyl ligand bonded to the metal through the benzo ring in an η^4 fanshion. It is found that the C_5 ring (C(34) to C(38)) and the C_6 ring (C(37) to C(42)) in **4** are bent away from the lithium and ytterbium atoms along the C(37)−C(38) line with a folding angle of 5.9°, to render possible formation of the Li−Cl, Yb−Cl, Li−C(35), and Li−C(36) bonds.

The Yb−C(C_5 ring) distances range from 2.680(6) to 2.826(6) Å, with an average of 2.744(6) Å. This distance is comparable to those found in ytterbium(II) complexes $[\eta^5$:η^1-$Me_2NCH_2CH_2C_9H_6]_2$Yb (2.722(10) Å),[14] *rac*-$(CH_2)_2(C_9H_6)_2$Yb(THF)$_2$ (2.699(4) Å),[24] $[\eta^5$:η^1-$Me_2NCH_2CH_2C_9H_5SiMe_3]_2$Yb (2.778(14) Å),[14] $(C_5H_9C_9H_6)_2$Yb(THF)$_2$ (2.776(7) and 2.76(6)

(18) Liang, H.; Shen, Q.; Jin, S.; Lin, Y. *J. Chem. Soc., Chem. Commun.* **1992**, 480−481.
(19) Hauber, S. O.; Niemeyer, M. *Inorg. Chem.* **2005**, *44*, 8644.
(20) Niemeyer, M. *Eur. J. Inorg. Chem.* **2001**, 1969.
(21) Shannon, R. D. *Acta Crystallogr.* **1976**, *A32*, 751.
(22) Burns, C. J.; Anderson, R. A. *J. Am. Chem. Soc.* **1987**, *109*, 915.
(23) Burns, C. J.; Anderson, R. A. *J. Am. Chem. Soc.* **1987**, *109*, 941.
(24) Tian, S.; Arredondo, V. M.; Stern, C. L.; Marks, T. J. *Organometallics* **1999**, *18*, 2568.

Table 1. Selected Bond Lengths (Å) and Angles (deg) for Complexes 4, 7, 8, and 9

4		7[a]		8[b]		9	
Yb−C14	2.777(6)	Sm−C8	2.751(4)	Nd−C8	2.776(13)	C3−C3A	1.371(4)
Yb−C15	2.683(6)	Sm−C9	2.637(4)	Nd−C9	2.669(12)	C1−C2	1.343(3)
Yb−C16	2.680(6)	Sm−C10	2.707(4)	Nd−C10	2.741(14)	C1−C5	1.468(3)
Yb−C17	2.755(6)	Sm−C11	2.974	Nd−C11	2.980(14)	C2−C3	1.463(3)
Yb−C18	2.826(6)	Sm−C12	2.991	Nd−C12	3.015(13)	C4−C5	1.408(3)
Yb−C37	3.221(6)	Sm−Ct1	2.545	Nd−Ct1	2.571	C4−C9	1.385(3)
Yb−C38	3.139(6)	Sm−C28	2.874(4)	Nd−C24	2.822(12)	C5−C6	1.369(3)
Yb−C39	2.903(6)	Sm−C29	2.713(4)	Nd−C25	2.748(13)	C6−C7	1.381(3)
Yb−C40	2.733(6)	Sm−C30	2.673(4)	Nd−C26	2.783(14)	C7−C8	1.379(3)
Yb−C41	2.772(6)	Sm−C31	2.879(4)	Nd−C27	2.969(15)	C8−C9	1.385(3)
Yb−C42	3.010(7)	Sm−C32	3.004	Nd−C28	3.001(13)		
Li−C34	2.882	Sm−Ct2	2.562	Nd−Ct2	2.599		
Li−C35	2.302	Sm−C48	2.793(4)	Nd−C40	2.887(12)		
Li−C36	2.259	Sm−C49	2.710(5)	Nd−C41	2.749(14)		
Li−C37	2.797	Sm−C50	2.743(5)	Nd−C42	2.721(13)		
		Sm−C51	2.943(4)	Nd−C43	2.888(12)		
		Sm−C52	2.978	Nd−C44	2.997(12)		
		Sm−Ct3	2.568	Nd−Ct3	2.584		
		Sm−N1	2.768(3)	Nd−N1	2.795(10)		
		Ct1−Sm−N1	91.5	Ct1−Nd−N1	91.0		
		Ct2−Sm−N1	107.6	Ct2−Nd−N1	103.5		
		Ct3−Sm−N1	103.8	Ct3−Nd−N1	107.5		
		Ct2−Sm−Ct1	115.2	Ct2−Nd−Ct1	115.1		
		Ct3−Sm−Ct1	115.2	Ct3−Nd−Ct1	115.2		
		Ct3−Sm−Ct2	118.6	Ct3−Nd−Ct2	119.2		

[a] Ct1 means the centroid of C8, C9, C10, C11, C12 ring; Ct2: C28, C29, C30, C31, C32 ring; Ct3: C48, C49, C50, C51, C52 ring. [b]Ct1 means the centroid of C8, C9, C10, C11, C12 ring; Ct2: C24, C25, C26, C27, C28 ring; Ct3: C40, C41, C42, C43, C44 ring.

Scheme 4

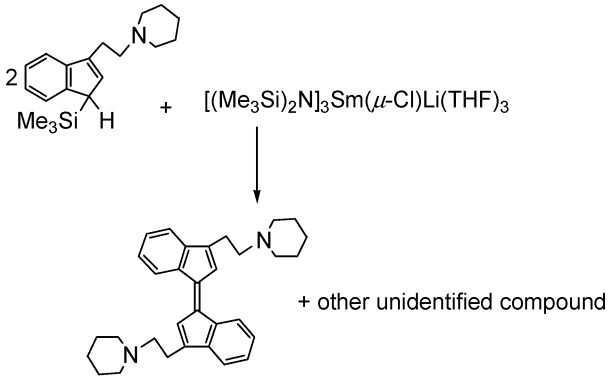

Scheme 5

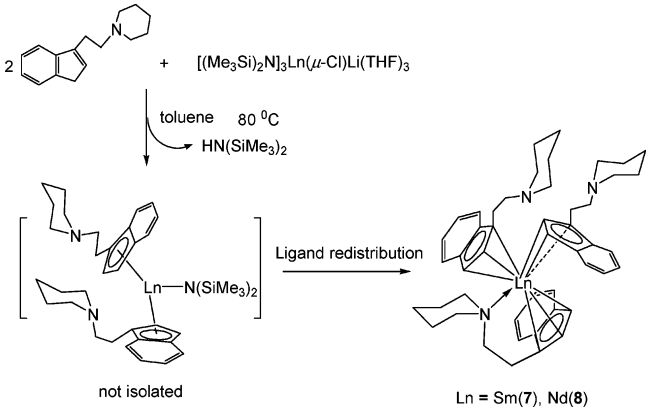

Å),[25] [η^5:η^1-$Me_2C(C_9H_6)(C_2B_{10}H_{10})$]Yb(DME)$_2$ (2.789(8) Å),[26] and [η^5:η^1-$Me_2Si(Me_2NCH_2CH_2C_9H_5)(HN^tBu)]_2$Yb (2.806(12) Å).[14] So, it should be assigned as an η^5-bonding mode.

An unexpected highly π-conjugated bis(*N*-piperidineethyl)-dibenzofulvalene, $(C_5H_{10}NCH_2CH_2C_9H_5)_2$ (**9**), was isolated as a byproduct in the preparation of **6**. Treatment of [$(Me_3Si)_2N]_3Sm^{III}(\mu$-Cl)Li(THF)$_3$ with 2 equiv of 1-Me_3Si-3-$C_5H_{10}NCH_2CH_2C_9H_6$ (**2**) also led to the isolation of **9** and other unidentified solids (Scheme 4). Compound **9** was fully characterized by NMR spectra, elemental analyses, and X-ray diffraction study (Figure 2). NMR analyses results suggested the presence of one indene and one substituted *N*-piperidineethyl groups. X-ray diffraction study revealed that the two *N*-piperidineethyl-functionalized indenyl ring is coupled through a C═C bond with a distance of 1.371(4) Å, which is longer than the standard 1.34 Å expected for the C═C bond in ethylene and other planar fulvalenes.[27] The C(3)−C(3a) distance of 1.371(4) Å is also slightly longer than that of 1.359(10) Å found in the π-conjugated fulvalene $C_{24}H_{12}(SiMe_3)_2$.[28] It is readily apparent from the crystallographic analysis that the C−C bond lengths in the conjugated fulvalene moiety of **9** alternate between long and short, and there is a significant double-bond localization between (C1)−C(2), C(3)−C(3A), and C(2A)−C(1A) (Table 1).

Evidence that a cyclopentadienyl radical is a key intermediate in oxidative coupling was provided by Sitzmann and co-workers, who recently reported the isolation and crystal structure of a pentasubstituted cyclopentadienyl radical.[29] This Cp radical, which was prepared by reaction of its corresponding anion with ferrous chloride, has the sterically hindering isopropyl substituents, which prevent it from coupling. A similar result was observed by Okuda and co-workers, who reported an oxidative coupling of a trimethylsilyl-substituted cyclopentadienide anion by iron(III) chloride.[30] Stradiotto et al. recently observed an

(25) Cui, D.; Tang, T.; Cheng, J. H.; Hu, N.; Chen, W.; Huang, B. *J. Organomet. Chem.* **2002**, *650*, 84.

(26) Wang, S.; Yang, Q.; Mak, T. C. W.; Xie, Z. *Organometallics* **2000**, *19*, 334.

(27) (a) Bartell, L. S.; Roth, E. A.; Hollewell, C. D.; Kuchitsu, K. S.; Young, J. E. *J. Chem. Phys.* **1965**, *26*, 2683. (b) Ishimori, M.; West, R.; Teo, B. K.; Dahl, L. F. *J. Am. Chem. Soc.* **1971**, *93*, 7101.

(28) Malaba, D.; Tessier, C. A.; Youngs, W. J. *Organometallics* **1996**, *15*, 2918.

(29) (a) Sitzmann, H.; Boese, R. *Angew. Chem., Int. Ed. Engl.* **1991**, *30*, 971. (b) Sitzmann, H.; Bock, H.; Boese, R.; Dezember, T.; Havlas, Z.; Kaim, W.; Moescherosch, M.; Zanathy, L. *J. Am. Chem. Soc.* **1993**, *115*, 12003.

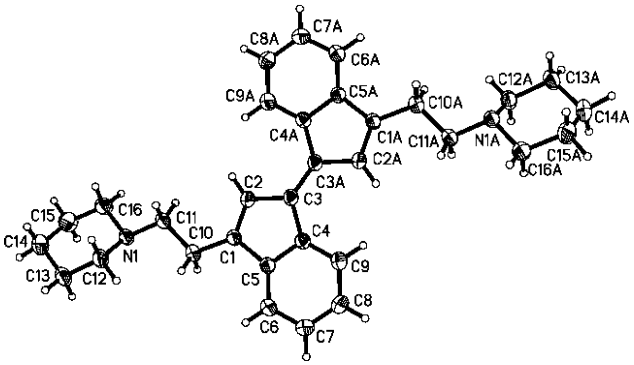

Figure 2. Molecular structure of **9**.

oxidative coupling in the study of [1,5]-silicon shifts in indenylsilanes leading to isolation and characterization of the dimer $[C_{18}H_{10}(SiMe_3)_2]_2$.[31]

Thus, the formation of **9** is proposed to go through a radical process initiated by homolysis of the Ln−N(SiMe$_3$)$_2$ (Ln = Eu, Sm) bond, which has been established in our previous works.[12−14] The radical •N(SiMe$_3$)$_2$ abstracts the hydrogen atom on the saturated carbon atom on the indene ring of 1-Me$_3$Si-3-C$_5$H$_{10}$NCH$_2$CH$_2$C$_9$H$_6$ (**2**), giving the radical 1-Me$_3$Si-3-C$_5$H$_{10}$NCH$_2$-CH$_2$C$_9$H$_5$•, which is then coupled to give (1-Me$_3$Si-3-C$_5$H$_{10}$-NCH$_2$CH$_2$C$_9$H$_5$)$_2$. Homolysis of the C−SiMe$_3$ bond[31] and electron rearrangement then leads to the isolated compound **9**, having two indenyl rings coupled through a C═C bond.

It has been documented that Sm^{3+}/Sm^{2+} and Nd^{3+}/Nd^{2+} have more negative reductive potentials than those of Yb^{3+}/Yb^{2+} and Eu^{3+}/Eu^{2+}. To study the ligands and the Ln^{3+}/Ln^{2+} reductive potentials' effects on the reactions, the interactions of the above indene compounds with the lanthanide(III) amides [(Me$_3$-Si)$_2$N]$_3$Ln(μ-Cl)Li(THF)$_3$ (Ln = Sm, Nd) were examined. Treatment of lanthanide(III) amides [(Me$_3$Si)$_2$N]$_3$Ln(μ-Cl)Li-(THF)$_3$ (Ln = Sm, Nd) with 2 equiv of C$_5$H$_{10}$NCH$_2$CH$_2$C$_9$H$_7$ (**1**) afforded novel trisindenyl lanthanide(III) complexes with general formula [η^3-C$_5$H$_{10}$NCH$_2$CH$_2$C$_9$H$_6$]$_2$Ln^{III}[η^3:η^1-C$_5$H$_{10}$-NCH$_2$CH$_2$C$_9$H$_6$] (Ln = Sm (**7**), Nd (**8**)) (Scheme 5). The complexes are air- and moisture-sensitive solids. They are soluble in toluene, benzene, and polar solvents such as THF, DME, and pyridine, but only slightly soluble in *n*-hexane. They were fully characterized by spectroscopic methods and elemental analyses. The structures of the complexes were additionally determined by X-ray diffraction study. ^{1}H NMR studies indicated that the protons of the indenyl rings resonated in the range 10.2 to 6.17 ppm for complex **7**, which is similar to the range of proton resonances for the indenyl ligands observed in (C$_9$H$_7$)$_3$Sm(THF),[32] and in the range 8.25 to 5.30 ppm for indenyl ligands for complex **8**. The protons of substituted groups of the indenyl rings resonated at the expected ranges subject to the paramagnetic properties of the complexes.

X-ray analyses revealed that the central metals in complexes **7** and **8** were coordinated by three indenyl ligands and one nitrogen atom of the substituted group (Figure 3 and Figure 4). The metal ions are situated at the center of the distorted pseudo-tetrahedron. The two complexes crystallize in the monoclinic system and belong to the same space group, $P2_1/n$. So, they are isomorphous. Selected bond lengths and angles are listed in Table 1.

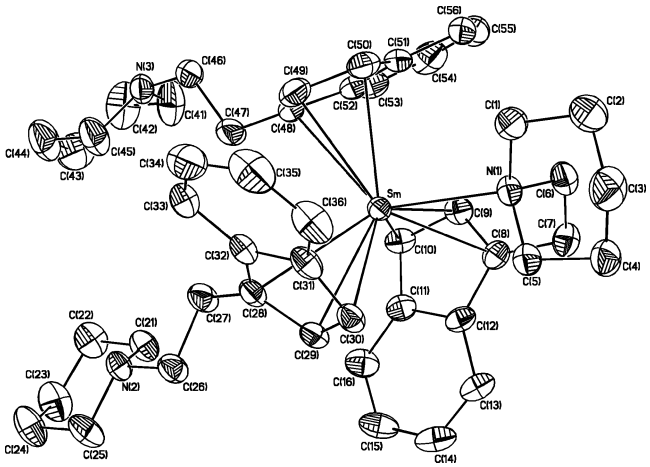

Figure 3. Molecular structure of **7**. Hydrogen atoms are omitted for clarity.

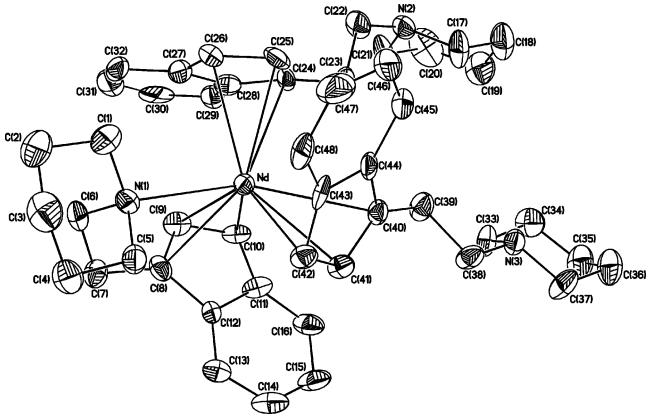

Figure 4. Molecular structure of **8**. Hydrogen atoms are omitted for clarity.

From Table 1, we can see that the two carbon atoms shared by both C$_5$ and C$_6$ rings of a substituted C$_9$H$_6$ ligand lie significantly more remote from the metal ion than the three carbon atoms belonging exclusively to the C$_5$ fragments, which are likely to approach a more allyl-like nature. However, the usual consequences of the decrease of the ionic radius of the Ln^{3+} ion when moving from Nd^{3+} to Sm^{3+} are clearly reflected by the average Ln−C, Ln−Ct (Ct = the centroid of the C$_5$ ring of indenyl ligands), and Ln−N distances.

The corresponding average Ln−C (Ln = Sm, Nd) and Ln−Ct (Ln = Sm, Nd) distances of 2.825(4) and 2.558 Å found in **7** and 2.849(13) and 2.585 Å found in **8** are also longer than the corresponding average Ln−C (Ln = Sm, Nd) and Ln−Ct (Ln = Sm, Nd) distances of 2.811(9) and 2.538 Å in (C$_9$H$_7$)$_3$-Sm(THF)[32] and 2.83(2) and 2.57 Å in (C$_9$H$_7$)$_3$Nd(THF).[32] The Sm−N(1) distance of 2.768(3) Å in **7** is also significantly longer than those of 2.301(3) Å in (C$_5$Me$_5$)$_2$SmN(TMS)$_2$[33] and 2.320-(4) Å in Me$_2$Si(C$_5$Me$_4$)(N^{t}Bu)SmN(TMS)$_2$;[34] these differences may be due to the combined effects of different ionic radii and the space-demanding nature of benzo groups of the three substituted indenyl ligands in the complexes. The Sm−N(1) and Nd−N(1) distances of 2.768(3) and 2.795(10) Å found in **7** and **8** are significantly longer than the Ce−N distance of 2.684(4) Å found in (C$_9$H$_7$)$_3$CePy;[35] these differences may be attributed

(30) Okuda, J.; Herdtweck, E.; Zeller, E. M. *Chem. Ber.* **1991**, *124*, 1575.
(31) Stradiotto, M.; Hazendonk, P.; Bain, A. D.; Brook, M. A.; McGlinchey, M. J. *Organometallics* **2000**, *19*, 590.
(32) Guan, J.; Shen, Q.; Fischer, R. D. *J. Organomet. Chem.* **1997**, *549*, 203.
(33) Evans, W. J.; Keyer, R. A.; Ziller, J. W. *Organometallics* **1993**, *12*, 2618.
(34) Tian, S.; Arredondo, V. M.; Stern, C. L.; Marks, T. J. *Organometallics* **1999**, *18*, 2568.
(35) Zazzetta, A.; Greco, A. *Acta. Crystallogr.* **1979**, *B35*, 457.

Table 2. Selected Bond Lengths and Angles from the DFT-Optimized Structure of 4, [4-Li]$^-$, 4-LiCl, 4′-LiCl, (η^5:η^5-Ind)$_2$Yb(NH$_3$)$_2$ (A), (η^5:η^6-Ind)$_2$Yb(NH$_3$)$_2$ (B), and [(η^5:η^6-Ind)$_2$Yb(NH$_3$)$_2$Li]$^+$ (C) (atom labeling refers to the X-ray structure of 4)

	4	[4-Li]$^-$	4-LiCl	4′-LiCl	A[a]	B	C
			Distances (Å)				
Yb−C14	2.758	2.757	2.763	2.713	2.732 2.736	2.721	2.671
Yb−C15	2.692	2.697	2.709	2.697	2.686 2.748	2.717	2.692
Yb−C16	2.720	2.718	2.707	2.703	2.732 2.736	2.721	2.671
Yb−C17	2.820	2.807	2.746	2.724	2.740 2.847	2.763	2.692
Yb−C18	2.847	2.834	2.784	2.741	2.740 2.847	2.763	2.692
Yb−C37	3.225	3.210	3.113	2.805		2.943	3.059
Yb−C38	3.313	3.113	3.027	2.792		2.943	3.059
Yb−C39	2.878	2.889	2.805	2.751		2.847	2.869
Yb−C40	2.729	2.741	2.651	2.699		2.751	2.714
Yb−C41	2.778	2.781	2.679	2.693		2.751	2.714
Yb−C42	3.004	2.996	2.879	2.753		2.847	2.869
Yb−Cl	2.729	2.675					
Yb−N1	2.692	2.710	2.714	2.604	2.561	2.556	2.644
Yb−N2	5.528	5.617	5.702	5.483	2.561	2.556	2.644
Li−Cl	2.286						
Li−C34	2.896						2.149
Li−C35	2.362						2.112
Li−C36	2.233						2.149
Li−C37	2.699						2.253
Li−C38	3.082						2.253
			Angles (deg)				
Cl−Yb−N1	92	90.9					
N2−Li−Cl	127						
HOMO/LUMO gap (eV)	0.73	0.73	0.92	1.02	0.59	0.73	0.61
relative energy (eV)					0	0.08	

[a] There are two symmetry-independent η^5-C$_5$ rings, thus two different series of Yb-(C14/C18) distances.

to the co-effects of the hybridization state of the nitrogen atoms, the ionic radii, and steric effects.

The formation of complexes **7** and **8** may be through silylamine elimination[36] followed by ligand redistribution reaction. It is different from the above reactivity pattern for the formation of an unexpected π-conjugated fulvalene (**9**) in the reaction of silyl-substituted indene (**2**) with [(Me$_3$Si)$_2$N]$_3$Sm-(μ-Cl)Li(THF)$_3$. The formation pathway for complexes **7** and **8** is proposed in Scheme 5.

The above results suggested that steric effects of ligands and Ln^{3+}/Ln^{2+} reductive potentials have a great influence on the reaction pattern. The interactions of non-silyl-substituted *N*-piperidineethyl-functionalized indene compounds with lanthanide(III) amides [(Me$_3$Si)$_2$N]$_3$Ln(μ-Cl)Li(THF)$_3$ (Ln = Yb, Eu) produced the indenyl lanthanide(II) complexes via silylamine elimination/homolysis of the Ln−N bond, while interactions of non-silyl-substituted *N*-piperidineethyl-functionalized indene (**1**) with lanthanide(III) amides [(Me$_3$Si)$_2$N]$_3$Ln(μ-Cl)Li(THF)$_3$ having more negative Ln^{3+}/Ln^{2+} (Ln = Sm, Nd) reductive potentials produced the tris-indenyl lanthanide(III) complexes via silylamine elimination reaction. Isolation and characterization of dibenzofulvalene **9** in cases of the interactions of silyl-substituted *N*-piperidineethyl-functionalized indene (**2**) with lanthanide amides [(Me$_3$Si)$_2$N]$_3$Ln(μ-Cl)Li(THF)$_3$ (Ln = Eu, Sm) suggested that the samarium, which has a more negative Sm^{3+}/Sm^{2+} reductive potential than that of Eu^{3+}/Eu^{2+}, may have a reaction pattern similar to europium, indicating the ligands' effects on the reaction. The interactions of sterically demanding silyl-substituted *N*-piperidineethyl-functionalized indene compound (**2**) with the lanthanide amides [(Me$_3$Si)$_2$N]$_3$Ln(μ-Cl)-Li(THF)$_3$ (Ln = Yb, Eu) produced the organolanthanide(II) complexes with indenyl ligands in a novel η^4-bonding mode, suggesting the steric effects on the coordination mode of indenyl ligands.

Theoretical Calculations. In order to understand the peculiar η^4 coordination mode of the metal in compound **4**, we have carried out a DFT analysis on this complex as well as on a series of related models. Complete geometry optimization of **4** leads to a structure that is close to the solid-state X-ray one, as exemplified by the major optimized metric data given in Table 2 (compare with Table 1). In particular, the η^4 coordination mode of the C$_6$ ring is also found by the calculations, with four short (2.73 to 3.00 Å) and two long (3.23 to 3.31 Å) Yb−C distances. The corresponding Mulliken overlap populations (OPs) indicate that the two "nonbonding" Yb−C contacts are in fact weakly bonding (small positive values), the four other Yb−C contacts exhibiting OPs that are significantly much larger.[17] These results suggest strongly that the metal in **4** is forced to bind to the C$_6$ ring in an η^4 fashion, whereas without any molecular strain it would prefer to bind it in an η^6 mode (or rather to the C$_5$ ring in an η^5 mode) in such a way that it would reach the 16-electron count, which usually provides stability to this type of complexes related to d^0 Cp$_2$ML$_2$ species. Although electron-deficient, the 14-electron complex **4** exhibits a significant HOMO/LUMO gap, as seen on its MO diagram shown in Figure 5. This diagram is fully consistent with the existence of a diamagnetic $4f^{14}$ Yb(II) center. The effect of the presence of the lithium atom coordinating one C−C bond of a C$_5$ ring can be tested by removing Li$^+$ from **4** and reoptimizing the structure of the remaining anion, namely, [(C$_5$H$_{10}$NCH$_2$CH$_2$-C$_9$H$_5$SiMe$_3$)$_2$ClYb]$^-$ ([**4-Li**]$^-$). A shortening by 5−6% of the Yb−C37 and Yb−C38 distances is obtained (Table 2). A

(36) Eppinger, J.; Spiegler, M.; Hieringer, W.; Herrmann, W. A.; Anwander, R. *J. Am. Chem. Soc.* **2000**, *122*, 3080.

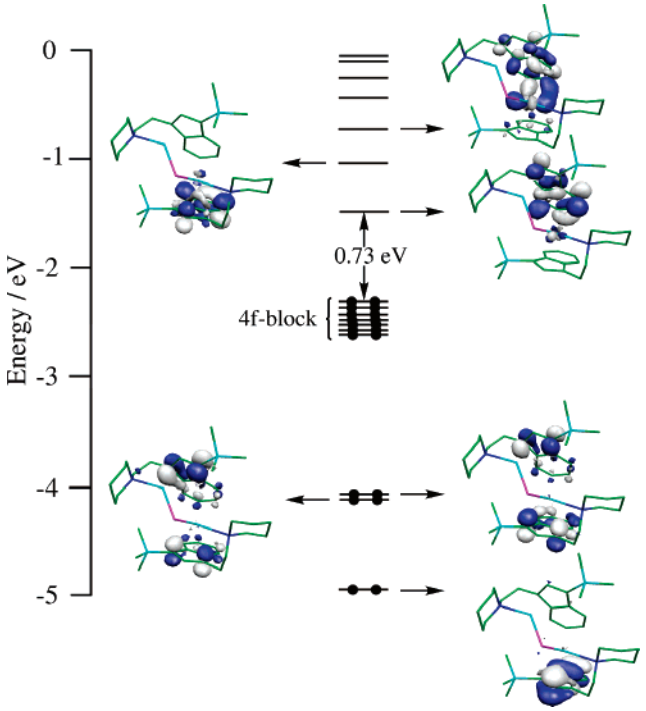

Figure 5. MO diagram of **4**.

similar reoptimization, but this time after removing the LiCl molecule from **4** and still keeping only one nitrogen atom (i.e., N1) bonded to Yb (model compound noted **4-LiCl**), leads to a shifting of the metal atom toward C37 and C38 (Table 2), indicating a distorted coordination mode approaching closer to the η^6 hapticity. The removal of the major steric effects in this latter model by changing the $SiMe_3$ groups into SiH_3 and the $C_5H_{10}N$ rings into NH_2 units, i.e., optimizing $(H_2NCH_2CH_2C_9H_5\text{-}SiH_3)_2Yb$ (model compound noted **4′-LiCl**), in the same local minimum, allows the metal to achieve the η^6 coordination mode, as indicated by the optimized Yb−C bond distances given in Table 2. These results confirm that strain, steric, and electronic effects are frustrating the Yb(II) center in **4**, which would like to bind in an η^6 mode to the C_6 ring (or in an η^5 mode to the C_5 ring) and that there is a soft potential linking the η^4 and η^6 coordination modes, without any energy barrier in between.

We have tested the ability of Yb(II) to bind to the C_6 ring of the indenyl ligands in calculating the $(\eta^5\text{-ind})_2Yb(NH_3)_2$ model (**A**) and comparing it to its $(\eta^6{:}\eta^5\text{-ind})_2Yb(NH_3)_2$ isomer (**B**). This simple model compound was chosen because it is isoelectronic and structurally related to compound **4.** The most relevant data are given in Table 2, in which the atoms are labeled in a manner similar to compound **4**. The optimized structures of C_s symmetry are shown in Figure 6. The $(\eta^6{:}\eta^5)$ isomer **B** is computed to be only 0.08 eV less stable than the $(\eta^5{:}\eta^5)$ isomer **A**, indicating the rather easy availability to coordinate the C_6 ring.[3b] As expected, the C_6 ring is not perfectly symmetrically η^6 bonded, exhibiting a slight distortion toward η^4, with the Yb−C37 and Yb−C38 distances being ∼5% longer than the average of the four others. Reoptimization of the whole molecule with the Yb−C40 and Yb−C41 distances forced to be constant and equal to 2.650 Å, i.e., forcing the η^4 coordination of the C_6 ring, results in a destabilization of only 0.21 eV, confirming the soft potential linking the η^6 and η^4 coordination modes. When a Li^+ cation is added to the $(\eta^5{:}\eta^6\text{-Ind})_2Yb(NH_3)_2$ isomer in a manner similar to that in **4**, i.e., complexing the available C_5 ring, the resulting $[(\eta^5{:}\eta^6\text{-Ind})_2Yb(NH_3)_2Li]^+$ optimized structure of C_s symmetry (model **C**) exhibits an η^3 coordination

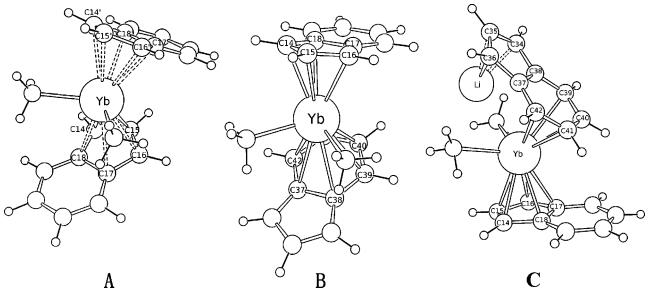

Figure 6. Optimized structures for $(\eta^5{:}\eta^5\text{-Ind})_2Yb(NH_3)_2$ (**A**), $(\eta^5{:}\eta^6\text{-Ind})_2Yb(NH_3)_2$ (**B**), and $[(\eta^5{:}\eta^6\text{-Ind})_2Yb(NH_3)_2Li]^+$ (**C**).

mode of the C_5 ring rather than the η^2 mode adopted by **4** (Figure 6 and Table 2). Nevertheless, Li^+ complexation of the C_5 ring has a similar effect as in **4** on the metal hapticity, namely, a distortion of the η^6 bonding mode toward the η^4 one.

MMA and ε-Caprolactone Polymerization. The catalytic activities of the complexes **4**−**8** as single-component MMA polymerization catalysts were examined. The polymerization procedures were carried out in a series of solvents. The product was quenched with acidified methanol after a fixed interval. The microstructure analyses of polymers were carried out using ^1H NMR and ^{13}C NMR spectra. The results are summarized in Table 4 and Table 5. It was found that π-bonded complexes **7** and **8** exhibit unexpected good catalytic activities on MMA polymerization, and complex **7** showed high catalytic activities on ε-caprolactone polymerization. It is also found that complexes **4**−**6** can function as single-component MMA polymerization catalysts with good catalytic activities. The results are listed in Table 3.

It is of interesting to note that the catalytic activities of the complexes **4**−**6** as single-component MMA polymerization catalysts and the polymers' molecular weights are temperature dependent. The catalytic activities of the complexes and the polymers' molecular weights increase as the polymerization temperatures decrease; the highest molecular weight ($M_n = 1.03 \times 10^5$) can be obtained by using catalyst **4** when the polymerization process was carried out at −60 °C in DME. The substituents on the indenyl ligands and ionic radii of the central metals of the complexes also have an influence on the activities of the catalysts. Complexes with the Me_3Si group on the indenyl ligands showed a relatively higher activity than complexes without the Me_3Si group on the indenyl ligands (for example, catalysts **4** and **6**). The larger the ionic radius of the central metal of the catalyst, the higher the catalytic activity of the catalyst (for example, catalysts **5** and **6**).

The solvents used for polymerization not only have an influence on the activities of the catalysts but also have an influence on the tacticity of the polymers. The syndiotactic-controlled polymers were obtained when the polymerization processes were carried out in polar solvents such as THF and DME. The isotactic-controlled polymers can be obtained when the polymerization procedures were carried out in toluene. The catalysts generally showed higher activities in polar solvents such as THF and DME than in toluene.

As rare examples of tris-indenyl lanthanide(III) complexes exhibiting catalytic activities on olefin and other polar monomer polymerization,[37] the π-bonded complexes **7** and **8** as single-component MMA polymerization catalysts were examined. The results indicated that they exhibited unexpected good catalytic activities in catalyzing MMA polymerization in the temperature range 30 to −30 °C in THF and DME for catalyst **7** and in THF for catalyst **8**, but catalyst **8** showed higher activities at

Table 3. Data for MMA Polymerization

				stereochem							
cat.	solvent	t	T (°C)	mm	mr	rr	$M_n \times 10^{-3}$	$M_w \times 10^{-3}$	M_w/M_n	conv (%)	activity $\times 10^{-4}$
4[a]	THF	30 min	0	0	43	57				39	3.9
		3 min	−30	16	29	55	77.78	142.63	1.83	71	70.68
		10 s	−60	12	31	57	65.88	130.88	1.99	88	15.77
	DME	30 min	0	16	30	54	32.00	51.41	1.61	13	1.31
		30 min	−30	17	31	52	50.02	106.52	2.13	51	5.02
		1 min	−60	0	29	71	103.51	186.91	1.81	73	222.69
	toluene	30 min	0	55	23	22	30.59	59.60	1.95	2	0.18
		30 min	−30	49	23	28	30.86	76.70	2.49	9	1.07
		30 min	−60	49	22	29	37.43	85.62	2.29	1	0.15
5[b]	THF	30 min	30	19	34	47	27.82	44.64	1.60	21	2.14
		30 min	10	13	32	55	32.68	68.22	2.09	34	3.37
		10 min	0	17	33	50	28.43	52.56	1.85	54	16.4
	DME	30 min	10	19	32	49	22.73	43.06	1.89	8	0.85
		30 min	0	18	32	50				29	2.90
		2 min	−30	25	31	44	39.96	88.89	2.22	51	76.05
		2 min	−60	16	30	54	52.29	106.94	2.05	86	124.5
	toluene	30 min	60	71	16	13	36.84	80.84	2.19	4	0.36
		30 min	30	77	13	10	73.10	135.17	1.85	7	0.71
6[b]	THF	30 min	10	20	32	48	47.26	77.048	1.63	14	1.39
		30 min	0	18	33	49				44	4.4
		10 s	−30	19	33	48	40.727	75.04	1.84	83	1482
		10 s	−60	12	34	54	50.56	89.22	1.76	95	1662
	DME	30 min	30	21	35	44	22.27	28.79	1.29	6	0.57
		30 min	0	20	31	49				22	2.14
		10 s	−30	17	33	50				65	1166
		10 s	−60	16	32	52	54.79	101.89	1.86	76	1379
	toluene	2 min	0	59	23	18	31.12	43.46	1.40	37	54.55
		30 s	−30	52	25	23	60.33	122.65	2.03	32	192.9
		30 s	−60	58	24	18	89.65	156.16	1.74	47	279.06
7[a]	THF	30 s	30	15	32	53	22.96	38.05	1.66	43	4.2
		30 s	0	13	30	57	33.47	57.35	1.71	41	4.17
		30 s	−30	10	31	59	75.84	137.24	1.81	36	3.59
		30 s	−60	11	28	61	84.16	158.73	2.42	24	2.42
	DME	30 s	30	16	32	52	16.71	23.08	1.38	9	0.96
		30 s	0	17	30	53	29.06	50.91	1.75	46	4.66
		30 s	−30	16	28	56				32	3.68
		30 s	−60	15	27	58	64.08	113.43	1.77	5	4.57
8[a]	THF	30 s	30	12	34	54	30.52	53.21	1.74	61	6.14
		25 s	10	15	40	45	36.70	75.73	2.06	61	7.29
		40 s	0	10	31	59				45	3.41
		40 s	−30	7	30	63				3	0.24
	DME	30 s	0	16	31	53	14.92	25.68	1.72	31	3.28
		3 s	−30	15	29	56	30.43	59.05	1.94	77	45.53
		3 s	−60	16	25	59				59	58.03

[a] Conditions: cat./MMA (mol/mol) = 1:500, MMA/solvent (v/v) = 1:5, activity: g PolyMMA/mol cat.·h; *t*: polymerization time; *T*: polymerization temperature. [b]Conditions: cat./MMA (mol/mol) = 1:500, MMA/solvent (v/v) = 1:3, activity: g PolyMMA/mol cat.·h; *t*.: polymerization time; *T*: polymerization temperature.

Table 4. Data for ε-Caprolactone (ε-CL) Polymerization[a]

cat.	solvent	time	T (°C)	$M_n \times 10^{-4}$	$M_w \times 10^{-4}$	M_w/M_n	conv (%)	activity $\times 10^{-4}$
7	THF		0					
		30 min	30	17.70	21.31	1.20	11	1.28
		5 min	60	28.21	41.49	1.47	41	27.7
	DME	2 min	30	33.76	60.02	1.78	58	98.02
		5 min	60	28.83	42.13	1.46	44	30.16
	toluene	1 min	30	44.18	58.28	1.32	56	190.3
		30 s	60	51.14	84.11	1.64	77	538.05

[a] Conditions: cat./ε-CL (mol/mol) = 1:500, ε-CL/solvent (v/v) = 1:5, activity: g Poly(ε-CL)/mol cat.·h; time: polymerization time; *T*: polymerization temperature.

lower temperatures in DME. The catalytic activity of these π-bonded complexes on MMA polymerization can be compared with those of lanthanide(II) complexes having donor-substituted groups on indenyl ligands.[12−15] The molecular weights of polymers increase as the polymerization temperatures decrease, indicating that the propagation process is favored at low temperatures. The syndiotactic-controlled polymers were obtained in all cases of MMA polymerization, and the molecular weight distributions are in a relative narrow range of 1.38 to 2.42.

The activity of the π-bonded complex **7** as a catalyst for ε-caprolactone polymerization was examined. It showed an unexpected high activity in catalyzing ε-caprolactone polymerization at a temperature ranging from 30 to 60 °C in DME

(37) (a) Yasuda, H. *J. Organomet. Chem.* **2002**, *647*, 128. (b) Hou, Z.; Wakatsuki, Y. *Coord. Chem. Rev.* **2002**, *231*, 1−22. (c) Nakayama, Y.; Yasuda, H. *J. Organomet. Chem.* **2004**, *689*, 4489. (d) Dehnicke, K.; Greiner, A. *Angew. Chem., Int. Ed.* **2003**, *42*, 1340−1354. (e) Deng, M. Y.; Yao, Y. M.; Shen, Q.; Zhang, Y.; Sun, J. *Dalton Trans.* **2004**, 944−950. (f) Kerton, F. M.; Whitwood, A. C.; Willans, C. E. *Dalton Trans.* **2004**, 2237−2244.

and toluene. The molecular weights of polymers increase as the polymerization temperatures increase; the highest molecular weight ($M_n = 51.14 \times 10^4$) and the highest catalytic activity (5.38×10^6 g pCL·(mol cat.)$^{-1}$·h^{-1}) are observed at 60 °C in toluene. The catalytic activity of complex **7** on ε-caprolactone polymerization is even higher than those of lanthanide(II) complexes with carbon-bridged biphenolate ligands[37e] or those of lanthanide(III) complexes with tetradentate dianionic ligands.[37f] The observed molecular weight distributions are in a narrow range of 1.20 to 1.78.

The MMA polymerization mechanism for the lanthanide(II) complexes **4**−**6** may be through a reductive dimerization of MMA to form a bis-intiator, comprising two lanthanide(III) enolates joined through their double bond.[38] However, the lanthanide(III) complexes **7** and **8** catalyzed MMA and ε-caprolactone polymerization may be through the coordination of the monomer to the metal center, leading to changes of the coordination mode of the indenyl ligand to η^1, which then initiated the polymerization process as the sterically crowded complex $(C_5Me_5)_3Sm$ did.[39]

Conclusion

In summary, the interactions of the *N*-piperidineethyl-functionalized indene compounds with lanthanide(III) amides $[(Me_3Si)_2N]_3Ln(\mu\text{-Cl})Li(THF)_3$ were studied. The results indicated that substituents on the indenyl ring have an influence on the reactivity and coordination mode of the indenyl ligands with the central metals. The interactions of the silyl-substituted *N*-piperidineethyl-functionalized indene compounds with the lanthanide(III) amides $[(Me_3Si)_2N]_3Ln^{III}(\mu\text{-Cl})Li(THF)_3$ (Ln = Yb, Eu) gave the lanthanide(II) complexes with the indenyl ligand coordinated to the metal through the benzo ring in a novel η^4-hapticity, which has been analyzed by DFT calculations, and an unexpected dibenzofulvalene in the cases of Ln = Eu and Sm. The interactions of non-silyl-substituted indene with the lanthanide(III) amides $[(Me_3Si)_2N]_3Ln^{III}(\mu\text{-Cl})Li(THF)_3$ produced lanthanide(II) complexes having an indenyl coordinated to the metal in a η^5-mode when Ln is Yb and Eu and tris-indenyl lanthanide(III) complexes with unusually long Ln−C and Ln−N distances having an allyl-like nature of the indenyl-to-metal coordination when the Ln^{3+}/Ln^{2+} has more negative reductive potentials (e.g., Ln = Sm, Nd). This work demonstrated that the homolysis of the Ln−N bond chemistry may be extended to samarium chemistry when a suitable sterically demanding ligand is applied. Theoretical calculations on ytterbium(II) complexes indicated that the strain, steric, and electronic effects have an influence on the hapticity of the indenyl ligands. The study on the catalytic activity of the complexes as single-component MMA polymerization catalysts showed that the π-bonded trisindenyl lanthanide(III) complexes showed unexpected good catalytic activity both on MMA and on ε-caprolactone polymerization. The temperatures, solvents, substituents, and catalytic conditions have an influence on the catalytic activities of the complexes.

Experimental Section

Materials and Methods. All syntheses and manipulations of air- and moisture-sensitive materials were carried out on flamed-dried Schlenk-type glassware on a Schlenk line. All solvents were refluxed and distilled over either finely divided $LiAlH_4$ or sodium benzophenone ketyl under argon prior to use unless otherwise noted. $CDCl_3$ was dried over activated 4 Å molecular sieves. MMA and ε-caprolactone (ε-CL) were dried over finely divided CaH_2, distilled before use. $[(Me_3Si)_2N]_3Ln^{III}(\mu\text{-Cl})Li(THF)_3$ (Ln = Yb, Eu, Sm, Nd) were prepared according to reported procedures.[14a,40] Elemental analysis data were obtained on a Perkin-Elmer 2400 Series II elemental analyzer. IR spectra were recorded on a Perkin-Elmer 983(G) spectrometer (CsI crystal plate, Nujol and Fluoroble mulls). Melting points were determined in sealed capillaries and are reported without correction. ^{1}H NMR and ^{13}C NMR spectra for analyses of compounds were recorded on a Bruker Avance-300 NMR spectrometer in pyridine-d_5 and benzene-d_6 for lanthanide complexes and in $CDCl_3$ for polymers and substituted indenes, and chemical shifts for ^{1}H and ^{13}C NMR spectra were referenced to internal solvent resonances. Gel permeation chromatography (GPC) analyses of polymer samples were carried at 30 °C using THF as eluent on a Waters-150C instrument and calibrated using monodispersed polystyrene standards at a flow rate of 1.0 mL·min^{-1}. Number-average molecular weights and polydispersities of polymers are given relative to PS standards. The polymers were analyzed according to the literature.[41]

Preparation of $C_5H_{10}NCH_2CH_2C_9H_7$ (1). To a solution of indene (12.0 mL, 102.0 mmol) in 100.0 mL of THF was slowly added a 1.53 M *n*-BuLi solution (67.8 mL, 102.0 mmol) at 0 °C. The reaction mixture was stirred at room temperature overnight and was then cooled to 0 °C. $C_5H_{10}NCH_2CH_2Cl$ (15.1 g, 102 mmol) was slowly added to the reaction mixture. The reaction mixture was stirred at room temperature overnight, and then it was hydrolyzed. The organic layer was separated and the aqueous layer was extracted with diethyl ether (2 × 15.0 mL). The organic fractions were combined and dried over anhydrous $MgSO_4$, filtered, and evaporated under vacuum. The oily, yellow product (14.2 g, 61%) was obtained after distillation under reduced pressure. ^{1}H NMR (300 MHz, $CDCl_3$): δ 7.49 (d, J = 7.28 Hz, 1H), 7.41 (d, J = 7.39 Hz, 1H), 7.23 (dd, J = 7.28 Hz, 5.24 Hz, 1H), 7.15 (dd, J = 7.39 Hz, 7.13 Hz, 1H), 6.26 (s, br, 1H), 3.34 (s, br, 2H) (C_9H_7), 2.81 (m, 2H), 2.71 (m, 2H) (CH_2CH_2), 2.53 (s, 4H), 1.68 (m, 4H), 1.51 (m, 2H) (C_5H_{10}). IR (Nujol and Fluoroble, cm^{-1}): ν 3066 (m), 2928 (m), 2854 (m), 1653 (s), 1559 (s), 1477 (s), 1451(s), 1308 (m), 1260 (m), 1227 (w), 1155 (m), 1113 (m), 1041(m), 992 (m), 961 (m), 915 (m), 864 (w), 769 (s), 714 (s), 663 (m), 559 (w). EIMS *m*/*z* (fragment, relative intensity %): 98 ($C_{16}H_{12}N^+$, 100), 115 ($C_9H_7^+$, 0.46), 128 ($C_9H_7CH_2^+$, 0.97), 227 (M^+, 2.13), 228 ($[M + 1]^+$, 0.19). HRMS/MALDI $[C_{16}H_{21}N + H]^+$: calcd 228.1752, found 228.1705.

Preparation of 1-Me_3Si-3-$C_5H_{10}NCH_2CH_2C_9H_6$ (2). To 50.0 mL of a THF solution of $C_5H_{10}NCH_2CH_2C_9H_7$ (**1**) (6.00 g, 26.4 mmol) was slowly added a 1.67 M *n*-BuLi solution (15.8 mL, 26.4 mmol) at 0 °C. The reaction mixture was stirred at room temperature overnight and was then cooled to 0 °C. To the mixture was added freshly distilled Me_3SiCl (6.70 mL, 52.8 mmol) in one portion. The reaction temperature was gradually raised to room temperature and stirred at that temperature overnight. The solvents and excess Me_3SiCl were evaporated under vacuum. Then 40.0 mL of *n*-hexane was added, and the precipitate was filtered off. The solvent was pumped off, affording the product as a yellow oil (5.96 g, 75%). ^{1}H NMR (300 MHz, $CDCl_3$): δ 7.47 (m, 2H), 7.31 (dd, J = 6.65, 7.92 Hz, 1H), 7.22 (dd, J = 6.65, 7.98 Hz, 1H), 6.35 (s, br, 1H), 3.41 (s, br, 1H) (C_9H_6), 2.87 (m, 2H), 2.70 (m, 2H) (CH_2CH_2), 2.53 (s, 4H), 1.68 (m, 4H), 1.50 (m, 2H) (C_5H_{10}), 0.05 (s, 9H) ($Si(CH_3)_3$). ^{13}C NMR (300 MHz, $CDCl_3$): δ 146.1, 144.3, 139.8, 130.5, 124.6, 123.7, 122.8, 118.9, 58.8 (C_9H_6), 54.7, 44.8, 26.1,

(38) (a) Boffa, L. S.; Novak, B. M. *Macromolecules* **1994**, *27*, 6993. (b) Ihara, E.; Morimoto, M.; Yasuda, H. *Macromolecules* **1995**, *28*, 7886.

(39) Evans, W. J.; Forrestal, K. J.; Ziller, J. W. *Angew. Chem., Int. Ed. Engl.* **1997**, *36*, 774.

(40) Zhou, S.; Wang, S.; Yang, G.; Liu, X.; Sheng, E.; Zhang, K.; Cheng, L.; Huang, Z. *Polyhedron* **2003**, *22*, 1019.

(41) Bovey, F. A.; Mirau, P. A. *NMR of Polymers*; Academic Press: San Diego, 1996.

25.4, 24.5 ($CH_2CH_2C_5H_{10}$), −2.4 ($Si(CH_3)_3$). IR (Nujol and Fluoroble, cm^{-1}): ν 3066 (s), 3012 (s), 2933 (s), 2853 (m), 1653 (m), 1559 (m), 1457 (s), 1448 (s), 1375 (m), 1248 (s), 1155 (m), 1116 (m), 1030 (s), 930 (w), 877 (s), 838 (s), 764 (s), 735 (m), 614 (s), 563 (w). Anal. Calcd for $C_{19}H_{29}NSi$: C, 76.19; H, 9.76; N, 4.68. Found: C, 76.56; H, 9.64; N, 5.00.

Preparation of [η^5:η^1-$C_5H_{10}NCH_2CH_2C_9H_6$]$_2$Yb^{II} (3). To a toluene (30.0 mL) solution of $[(Me_3Si)_2N]_3Yb^{III}(\mu\text{-Cl})Li(THF)_3$ (1.18 g, 1.30 mmol) at room temperature was slowly added a toluene (10.0 mL) solution of $C_9H_7CH_2CH_2NC_5H_{10}$ (**1**) (0.590 g, 2.60 mmol). After the reaction was stirred at room temperature for 6 h, the mixture was then refluxed for 24 h until the color of the solution changed from yellow to purple-red. The solvent was evaporated under reduced pressure. The residue was washed with *n*-hexane (10.0 mL). The resulting solid was extracted with toluene (2 × 10.0 mL). The toluene solution was combined and concentrated to 15 mL, and purple-red needle crystals were obtained by cooling the concentrated solution at 0 °C (0.481 g, 59%). Mp: 154−156 °C. IR (Nujol and Fluoroble, cm^{-1}): ν 2933 (s), 2851 (m), 2802 (m), 2765 (w), 1684 (w), 1653 (s), 1559 (s), 1457 (s), 1262 (w), 1123 (s), 1033 (m), 760 (s). ^{1}H NMR (300 MHz, benzene-d_6): δ 7.53−7.34 (m, 8H), 6.26 (m, 2H), 6.18 (m, 2H) (C_9H_6), 2.86 (m, 4H), 2.75 (m, 4H), 2.46 (m, 8H), 1.68 (m, 8H), 1.47 (m, 4H) ($CH_2CH_2C_5H_{10}$). Anal. Calcd for $C_{32}H_{40}N_2Yb$: C, 61.42; H, 6.44; N, 4.48. Found: C, 61.74; H, 6.58; N, 4.17.

Preparation of [η^4:η^2:η^1-($C_5H_{10}NCH_2CH_2C_9H_5SiMe_3$)Li($\mu$-Cl)]Yb^{II}($\eta^5$:$\eta^1$-$C_5H_{10}NCH_2CH_2C_9H_5SiMe_3$) (4). To a toluene (30.0 mL) solution of $[(Me_3Si)_2N]_3Yb^{III}(\mu\text{-Cl})Li(THF)_3$ (1.36 g, 1.50 mmol) at room temperature was slowly added a toluene (10.0 mL) solution of 1-Me_3Si-3-$C_5H_{10}NCH_2CH_2C_9H_6$ (**2**) (0.90 g, 3.0 mmol). After the reaction was stirred at room temperature for 6 h, the mixture was then heated to 80 °C and the color of the solution changed from yellow to dark red. The mixture was then stirred at this temperature for 24 h. The solvent was evaporated under reduced pressure. The residue was washed with *n*-hexane (10.0 mL). The resulting solid was extracted with *n*-hexane (3 × 5 mL). The solution was combined and concentrated. The complex was isolated as dark red crystals (0.650 g, 54%) at room temperature after several days from the *n*-hexane solution. Mp: 192−194 °C. IR (Nujol and Fluoroble, cm^{-1}): ν 2934 (s), 2798 (m), 1634 (m), 1451 (s), 1381 (s), 1248 (s), 1155 (m), 1116 (m), 1030 (m), 877 (m), 839 (s), 763 (m), 735 (w), 614 (m). ^{1}H NMR (300 MHz, benzene-d_6): δ 9.27 (s, br, 1H), 8.14 (s, br, 1H), 7.73 (m, 2H), 7.47−7.13 (m, 4H), 6.18 (s, br, 2H) (C_9H_5), 3.19 (m, 4H), 2.75 (m, 4H), 2.47 (m, 8H), 1.66 (m, 4H), 1.45 (m, 4H), 1.34 (m, 2H), 1.21 (m, 2H) ($CH_2CH_2C_5H_{10}$), 0.39 (m, 9H) ($Si(CH_3)_3$), 0.20 (m, 9H) ($Si(CH_3)_3$). ^{1}H NMR (300 MHz, pyridine-d_5): δ 8.15−8.02 (br, 2H), 7.40−7.33 (m, 2H), 7.20−7.09 (m, 4H), 6.47 (s, 2H) (C_9H_5), 2.90 (m, 4H), 2.69 (m, 4H), 2.52 (m, 8H), 1.56 (m, 8H), 1.35 (m, 4H) ($CH_2CH_2C_5H_{10}$), −0.03 (s, 18H) ($Si(CH_3)_3$). Anal. Calcd for $C_{38}H_{56}N_2ClLiSi_2Yb$: C, 56.18; H, 6.95; N, 3.45. Found: C, 55.93; H, 7.04; N, 3.12.

Preparation of [η^5:η^1-$C_5H_{10}NCH_2CH_2C_9H_6$]$_2$Eu (5). To a toluene (30.0 mL) solution of $[(Me_3Si)_2N]_3Eu^{III}(\mu\text{-Cl})Li(THF)_3$ (1.09 g, 1.20 mmol) at room temperature was slowly added a toluene (10.0 mL) solution of $C_5H_{10}NCH_2CH_2C_9H_7$ (**1**) (0.560 g, 2.50 mmol). After the reaction was stirred at room temperature for 6 h, the temperature was raised to 50 °C and the reaction mixture was stirred at this temperature for 24 h. The solvent was evaporated under reduced pressure. The residue was washed with *n*-hexane (10.0 mL). The resulting solid was extracted with toluene (2 × 10.0 mL). The toluene solution was combined and concentrated to 15.0 mL to give a yellow, crystalline solid (0.560 g, 75%). Mp: 168−170 °C. IR (Nujol and Fluoroble, cm^{-1}): ν 2933 (m), 2852 (w), 2801 (w), 1653 (m), 1559 (s), 1457 (s), 1303 (w), 1258 (w), 1156 (w), 1106 (w), 1033 (w), 968 (w), 768 (m), 714 (w). Anal. Calcd for $C_{32}H_{40}N_2Eu$: C, 63.56; H, 6.67; N, 4.63. Found: C, 63.21; H, 6.37; N, 4.53.

Preparation of [η^4:η^2:η^1-($C_5H_{10}NCH_2CH_2C_9H_5SiMe_3$)Li($\mu$-Cl)]Eu($\eta^5$:$\eta^1$-$C_5H_{10}NCH_2CH_2C_9H_5SiMe_3$) (6). This compound was prepared as a yellow solid in 50% yield from reaction of $[(Me_3Si)_2N]_3Eu^{III}(\mu\text{-Cl})Li(THF)_3$ (1.25 g, 1.40 mmol) and 1-Me_3Si-3-$C_5H_{10}NCH_2CH_2C_9H_6$ (**2**) (0.840 g, 2.80 mmol) following procedures similar to those used for the preparation of complex **4**. Mp: 152−154 °C. IR (Nujol and Fluoroble, cm^{-1}): ν 3059 (w), 2934 (m), 2853 (m), 2757 (w), 1636 (w), 1457 (s), 1248 (s), 1151 (w), 1119 (w), 1033 (w), 878 (w), 839 (m), 763 (m), 698 (w), 612 (w). Anal. Calcd for $C_{38}H_{56}N_2ClEuLiSi_2$: C, 57.66; H, 7.13; N, 3.54. Found: C, 57.30; H, 6.63; N, 3.13.

$[C_5H_{10}NCH_2CH_2C_9H_5]_2$ (**9**) can be isolated as a byproduct from the reaction.

Preparation of [η^3-$C_5H_{10}NCH_2CH_2C_9H_6$]$_2$Sm^{III}[η^3:η^1-C_5H_{10}-$NCH_2CH_2C_9H_6$] (7). To a toluene (30.0 mL) solution of $[(Me_3Si)_2N]_3Sm^{III}(\mu\text{-Cl})Li(THF)_3$ (1.16 g, 1.30 mmol) at room temperature was slowly added a toluene (10.0 mL) solution of C_5H_{10}-$NCH_2CH_2C_9H_7$ (**1**) (0.590 g, 2.60 mmol). After the reaction was stirred at room temperature for 6 h, the temperature was raised to 80 °C and the reaction mixture was stirred at this temperature for 12 h. The solvent was evaporated under reduced pressure. The residue was washed with *n*-hexane (10.0 mL). The resulting solid was extracted with toluene (2 × 10.0 mL). The toluene solution was combined and concentrated to 15.0 mL. Orange-red crystals were obtained by cooling the concentrated solution at 0 °C (0.780 g, 72%). Mp: 208−210 °C. ^{1}H NMR (300 MHz, benzene-d_6): δ 10.02 (d, J = 8.13 Hz, 1H), 9.58 (d, J = 8.07 Hz, 1H), 8.91 (s, br, 1H), 8.60 (s, br, 1H), 8.25 (s, br, 1H), 8.02 (s, br, 1H), 7.88 (m, 1H), 7.47−7.34 (m, 5H), 6.83 (s, br, 2H), 6.73 (s, br, 2H), 6.17 (s, br, 2H) (C_9H_6), 3.19−2.46 (m, 24H), 1.84−0.34 (m, 18H) (CH_2CH_2-NC_5H_{10}). IR (Nujol and Fluoroble, cm^{-1}): ν 3066 (w), 2933 (m), 2853 (w), 2765 (w), 1653 (m), 1559 (m), 1457 (w), 1307 (w), 1254 (w), 1156 (w), 1111 (m), 1037 (w), 951 (w), 857 (w), 769 (m), 718 (m). Anal. Calcd for $C_{48}H_{60}N_3Sm$: C, 69.51; H, 7.29; N, 5.07. Found: C, 69.17; H, 7.13; N, 5.17.

Preparation of [η^3-$C_5H_{10}NCH_2CH_2C_9H_6$]$_2$Nd^{III}[η^3:η^1-C_5H_{10}-$NCH_2CH_2C_9H_6$] (8). This complex was prepared as blue crystals in 62% yield from reaction of $[(Me_3Si)_2N]_3Nd^{III}(\mu\text{-Cl})Li(THF)_3$ (1.07 g, 1.20 mmol) and $C_5H_{10}NCH_2CH_2C_9H_7$ (**1**) (0.550 g, 2.40 mmol) following procedures similar to those used for the preparation of complex **7**. Mp: 200−202 °C. ^{1}H NMR (300 MHz, benzene-d_6): δ 8.25 (d, J = 8.04 Hz, 2H), 7.81−7.40 (m, 10H), 6.78 (m, 1H), 5.95 (m, 1H), 5.75 (m, 1H), 5.30 (s, 3H) (C_9H_6), 3.05−2.16 (m, 24H), 1.88−0.20 (m, 18H) ($CH_2CH_2NC_5H_{10}$). IR (Nujol and Fluoroble, cm^{-1}): ν 2933 (m), 2853 (w), 2799 (w), 1653 (m), 1636 (w), 1457 (m), 1442 (w), 1397 (w), 1307 (w), 1258 (w), 1147 (w), 1114 (m), 1033 (w), 959 (w), 857 (w), 769 (m), 718 (m). Anal. Calcd for $C_{48}H_{60}N_3Nd$: C, 70.03; H, 7.35; N, 5.11. Found: C, 70.87; H, 7.34; N, 4.37.

Preparation of [$C_5H_{10}NCH_2CH_2C_9H_5$]$_2$ (9). This compound was prepared in 26% yield as brown crystals from a reaction of $[(Me_3Si)_2N]_3Sm^{III}(\mu\text{-Cl})Li(THF)_3$ (1.11 g, 1.20 mmol) and 1-Me_3-Si-3-$C_5H_{10}NCH_2CH_2C_9H_6$ (**2**) (0.740 g, 2.40 mmol) following procedures similar to those used for the preparation of complex **7**. ^{1}H NMR (300 MHz, $CDCl_3$): δ 7.93 (s, 2H), 7.31−7.18 (m, 8H) (C_9H_5), 2.88 (m, 4H), 2.77 (m, 4H) (CH_2CH_2), 2.54 (m, 8H), 1.64 (m, 8H), 1.58 (m, 4H) (NC_5H_{10}). Anal. Calcd for $C_{32}H_{38}N_2$: 85.29; H, 8.50; N, 6.21. Found: C, 84.93; H, 8.32; N, 6.09.

An unidentified solid can be isolated from the reaction mixture.

X-ray Crystallography. A suitable crystal of the complexes **4**, **7**, **8**, and **9** was mounted in a sealed capillary. Diffraction was performed on a Siemens SMART CCD-area detector diffractometer using graphite-monochromated Mo Kα radiation (λ = 0.71073 Å); temperature 293(2) K; ψ and ω scan technique; SADABS effects and empirical absorption were applied in the data corrections. All

Table 5. X-ray Experimental Data of Compounds 4, 7, 8, and 9

	4	7	8	9
empirical formula	$C_{38}H_{56}ClLiN_2Si_2Yb$	$C_{48}H_{60}N_3Sm$	$C_{48}H_{60}N_3Nd$	$C_{32}H_{38}N_2$
molecular mass	812.46	829.34	823.23	450.64
cryst syst	triclinic	monoclinic	monoclinic	triclinic
space group	$P\bar{1}$	$P2_1/n$	$P2_1/n$	$P\bar{1}$
a (Å)	11.8171(2)	14.5740 (5)	14.5822(2)	5.5969(15)
b (Å)	13.1286(2)	18.7396(2)	18.7434(6)	10.970(3)
c (Å)	14.4153(2)	16.4420 (2)	16.4400(4)	11.163(3)
α (deg)	72.8130(10)			70.031(4)
β (deg)	70.4390(10)	113.5500(10)	113.3030(10)	86.755(5)
γ (deg)	75.3670(10)			89.162(5)
V (Å^3)	1983.68(5)	4116.56(4)	4126.84(18)	643.1
temperature (K)	293(2)	293(2)	293(2)	294(2)
D_{calcd} (g cm^{-3})	1.360	1.338	1.325	1.164
Z	2	4	4	1
F(000)	832	1724	1716	244
no. of reflns collected	10 255	12 452	12 577	3661
no. of unique reflns	6892 ($R_{int} = 0.031$)	7140 ($R_{int} = 0.026$)	6146 ($R_{int} = 0.078$)	2600 ($R_{int} = 0.020$)
no. of params	406	469	469	154
λ (Å) Mo Kα	0.71073	0.71073	0.71073	0.71073
μ (mm^{-1})	2.512	1.462	1.294	0.067
θ limits (deg)	1.65/25.04	1.73/25.03	1.87/24.00	1.94/26.63
GOF	1.103	1.126	1.098	1.002
R ($I > 2\sigma(I)$)	0.043	0.038	0.086	0.056
wR_2	0.096	0.072	0.233	0.127
largest diff peak and hole (e·Å^{-3})	1.062 and −0.978	0.628 and −0.809	0.712 and −0.831	0.145 and −0.152

structures were solved by direct methods (SHELXS-97),[42] completed by subsequent difference Fourier syntheses, and refined by full-matrix least-square calculations based on F^2 (SHELXS-97).[42] The X-ray experimental data are given in Table 5. CCDC No. 252064 for **4**, 617100 for **9**, 617101 for **8**, and 617102 for **7** in CIF format have been deposited with the Cambridge Crystallographic Data Centre.

MMA and ε-Caprolactone Polymerization. MMA or ε-caprolactone polymerization reactions were performed in a 50.0 mL Schlenk flask, placed in an external temperature-controlled bath, on a Schlenk line, or in a glovebox. In a typical procedure the catalyst (20−50 mg) was loaded into the Schlenk flask and the solvent was added. After the external bath temperature was stabilized, MMA or ε-caprolactone was added through a gastight syringe. The polymer product was precipitated into methanol (50.0 mL), washed with methanol, and then dried to a constant weight in a vacuum oven at 50 °C. The stereochemistry of the polymers and their molecular weights were analyzed by ^{1}H NMR spectroscopy and GPC techniques, respectively.

Computational Details. DFT calculations were carried out using the Amsterdam Density Functional package[43] developed by Baerends and co-workers.[44] The local density approximation for electron correlation was treated with the Vosko−Wilk−Nusair parametrization.[45] The nonlocal corrections of Becke[46] and Perdew[47] (BP86) were added to the exchange and correlation energies, respectively. The numerical integration procedure applied for the calculations was developed by te Velde et al.[44e] The standard ADF STO TZP basis set was used.[43] The frozen-core approximation[48] was considered for Yb, 5p; Cl, 2p; Si, 2p; N, 1s; and C, 1s. Relativistic corrections were added using the ZORA (zeroth-order regular approximation) scalar Hamiltonian.[49] Geometry optimizations for (η^5:η^5-Ind)$_2$Yb(NH$_3$)$_2$, (η^5:η^6-Ind)$_2$Yb(NH$_3$)$_2$, and [(η^5:η^6-Ind)$_2$Yb(NH$_3$)$_2$Li]$^+$ were done with C_s symmetry as constraint.

Acknowledgment. We thank the National Natural Science Foundation of China (20472001, 20672002), the program for the NCET (NCET-04-0590), the Excellent Young Scholars Foundation of Anhui Province (04046079), and the Education Department of Anhui Province for financial support for this work. The theoretical investigation was supported by the Franco/Chilean grant CNRS/CONICYT 18176. Computing facilities were provided by the University of Rennes 1 (PCIO) and the IDRIS-CNRS national center. Professor Zixiang Huang is gratefully acknowledged for his help in the X-ray structure determination.

Supporting Information Available: Tables giving Cartesian coordinates for the optimized structures in XYZ format and CIF files giving X-ray crystallographic data for the structure determination of complexes **4**, **7**, **8**, and **9**. This material is available free of charge via the Internet at http://pubs.acs.org.

OM060979I

(42) Sheldrick, G. M. *SHELXTL*, version 5.10; Bruker Analytical X-ray Systems, Inc.: Madison, WI, 1997.

(43) *ADF2002.01, Theoretical Chemistry*; Vrije Universiteit: Amsterdam, The Netherlands, SCM (http://www.scm.com).

(44) (a) Baerends, E. J.; Ellis, D. E.; Ros, P. *Chem. Phys.* **1973**, *2*, 41. (b) te Velde, G.; Baerends, E. J. *J. Comput. Phys.* **1992**, *99*, 84. (c) Guerra, C. F.; Snijders, J. G.; te Velde, G.; Baerends, E. J. *Theor. Chim. Acc.* **1998**, *99*, 391. (d) Bickelhaupt, F. M.; Baerends, E. J. *Rev. Comput. Chem.* **2000**, *15*, 1. (e) Velde, G. Te; Bickelhaupt, F. M.; Guerra, C. F.; Van Gisbergen, S. J. A.; Baerends, E. J.; Snijders, J. G.; Ziegler, T. *J. Comput. Chem.* **2001**, *22*, 931.

(45) Vosko, S. D.; Wilk, L.; Nusair, M. *Can. J. Chem.* **1990**, *58*, 1200.

(46) (a) Becke, A. D. *J. Chem. Phys.* **1986**, *84*, 4524. (b) Becke, A. D. *Phys. Rev. A* **1988**, *38*, 3098.

(47) (a) Perdew, J. P. *Phys. Rev. B* **1986**, *33*, 8822. (b) Perdew, J. P. *Phys. Rev. B* **1986**, *34*, 7406.

(48) Verluis, L.; Ziegler, T. *J. Chem. Phys.* **1988**, *88*, 322.

(49) (a) Van Lethe, E.; Baerends, E. J.; Snijders, J. G. *J. Chem. Phys.* **1993**, *99*, 4597. (b) Van Lethe, E.; Baerends, E. J.; Snijders, J. G. *J. Chem. Phys.* **1994**, *101*, 9783. (c) Van Lethe, E.; Van Leeuwen, R.; Baerends, E. J.; Snijders, J. G. *Int. J. Quantum Chem.* **1996**, *57*, 281.